Virus Research 263 (2019) 47–54

Contents lists available at ScienceDirect

Virus Research

journal homepage: www.elsevier.com/locate/virusres

In vitro growth kinetics and gene expression analysis of the turkey adenovirus 3, a siadenovirus

Zeinab R. Aboezz[a], Hassan M. Mahsoub[b,c,*], Gabr El-Bagoury[a], F. William Pierson[d]

[a] Virology Department, Faculty of Veterinary Medicine, Benha University, Moshtahar, Toukh, Qalubiya, 13736, Egypt
[b] Department of Biomedical Sciences and Pathobiology, Virginia-Maryland College of Veterinary Medicine, Virginia Tech, Blacksburg, VA, 24061, United States
[c] Poultry Production Department, Faculty of Agriculture, Alexandria University, El-Shatby, Alexandria, 21545, Egypt
[d] Department of Population Health Sciences, Virginia-Maryland College of Veterinary Medicine, Virginia Tech, Blacksburg, VA, 24061, United States

ARTICLE INFO

Keywords:
Turkey adenovirus 3
Turkey hemorrhagic enteritis
Siadenovirus
Growth kinetics
Gene expression

ABSTRACT

Turkey adenovirus 3 (TAdV-3) belongs to the genus *Siadenovirus*, family *Adenoviridae*. Previously, nucleotide sequencing and annotation of the Virginia avirulent strain (VAS) of TAdV-3 genome, isolated in our laboratory, indicated the presence of a total of 23 genes and open reading frames (ORFs). The goals of this study were 1) to delineate the growth kinetics of the virus using a qPCR-based infectivity assay, and 2) to determine the virus gene expression profile during the early and late phases of infection in target B lymphocytes. The one-step growth curve experiment demonstrated 3 phases of virus replication cycle: a lag phase lasted for 12–18 h post-infection (h.p.i.), in which the virus titer declined; a log phase from 18 to 120 h.p.i., in which the number of infectious virus particles increased over 20,000 folds, and a brief decline phase thereafter. Southern blot analysis indicated that the synthesis of new viral DNA started by 8 h.p.i. Gene-specific RT-PCR analysis revealed the expression of mRNAs from the 23 TAdV-3 genes/ORFs. According to the temporal transcriptional profiling of TAdV-3 genome, genes could be divided into 3 groups based on the time of transcription initiation: group 1 showed detectable levels of transcription at 2 h.p.i and included 7 genes, *i.e.*, hyd, III, pX, pVI, II, 100 K, and 33 K; group 2 included 12 genes whose mRNAs were detected for the first time at 4 h.p.i., *i.e.*, ORF1, IVa2, pol, pTP, pIIIa, EP, DBP, E3, U exon, IV, ORF7, and ORF8; group 3 of transcripts were detectable starting 8 h.p.i. and included only 4 genes, *i.e.*, 52 K, 22 K, pVII, and pVIII. Our data suggest that the transcriptional kinetics of genus *Siadenovirus* differ from that observed in other adenoviral genera; however, a few TAdV-3 genes showed similar expression patterns to their adenoviral homologs.

1. Introduction

Turkey adenovirus 3 (TAdV-3), more commonly known as turkey hemorrhagic enteritis virus (THEV), is the causative agent of a variety of clinical conditions in a number of avian species. TAdV-3 causes hemorrhagic enteritis in turkeys, marble spleen disease in pheasants, and avian adenovirus splenomegaly in chickens (Pierson and Fitzgerald, 2013). TAdV-3 targets IgM-bearing B lymphocytes, inducing apoptosis and transient immunosuppression, which often results in additional mortality due to secondary bacterial infection (Pierson and Fitzgerald, 2013; Pierson et al., 1996; Rautenschlein et al., 2000; Saunders et al., 1993; Suresh and Sharma, 1995, 1996). TAdV-3 has a non-enveloped, icosahedral capsid of 70–90 nm in diameter, enclosing a linear, non-segmented, double-stranded DNA (dsDNA) genome of ~26 kb (Beach et al., 2009; Iltis et al., 1977; Jucker et al., 1996; Tolin and Domermuth, 1975; van den Hurk, 1992). TAdV-3 belongs to the family *Adenoviridae,* genus *Siadenovirus,* species Turkey siadenovirus A (Adams et al., 2014). TAdV-3 and frog adenovirus 1 (FrAdV-1) have been the only two members in the genus until 2009. Since then, several siadenovirus members have been recognized and associated with infections in different avian and non-avian species (Katoh et al., 2009; Kovács and Benkő, 2009; Kovács et al., 2010; Rivera et al., 2009; Wellehan et al., 2009).

The first siadenoviral genome to be partially and fully sequenced was TAdV-3 (Beach et al., 2009; Jucker et al., 1996; Pitcovski et al., 1998), followed by FrAdV-1 (Davison et al., 2000) and other

Abbreviations: TAdV-3, turkey adenovirus 3; VAS, Virginia avirulent strain; ORFs, open reading frames; h.p.i., hour(s) post-infection; pol, adenovirus DNA-dependent DNA polymerase; IPV, infectious viral particle(s)

* Corresponding author at: Center for One Health Research, Virginia-Maryland College of Veterinary Medicine, Virginia Tech, 1410 Prices Fork Rd., Blacksburg, VA 24061, United States.
E-mail address: hmahsoub@vt.edu (H.M. Mahsoub).

https://doi.org/10.1016/j.virusres.2019.01.005
Received 3 September 2018; Received in revised form 17 November 2018; Accepted 9 January 2019
Available online 10 January 2019
0168-1702/

siadenoviral species emerged recently (see references above). Computational analysis of the TAdV-3 genome indicated the presence of 23 genes/ORFs, 16 of which are homologous to the family common genes located at the expected genomic positions, *i.e.*, IVa2, DNA-dependent DNA polymerase (pol), pTP, 52 K, pIIIa, III (penton base), pVII, pX, pVI, II (hexon), endoprotease (EP), DNA-binding protein (DBP), 100 K, 33 K, pVIII, and IV (fiber). Two additional ORFs found in other, but not all, adenoviruses were also detected, *i.e.*, 22 K and U exon. The remaining 5 ORFs are putative and genus-specific, *i.e.*, ORF1, hyd, E3, ORF7, and ORF8 (Beach et al., 2009; Davison et al., 2003). The transcription of adenoviruses have been extensively studied with genus *Mastadenovirus*, which contains all human and some animal adenoviruses. Similar to other dsDNA viruses, some adenoviral genes are transcribed from the upper (or right, *r*) strand and some from the lower (or left, *l*) strand. In case of genus *Siadenovirus*, sequence analysis showed that the majority of gene are transcribed from the *r* strand, and a few genes, *i.e.*, IVa2, pol, pTP, DBP, U exon, and ORF8, are transcribed from the *l* strand (Davison and Harrach, 2011; Davison et al., 2003). The TAdV-3 structural proteins composing the virion and those interacting with the viral genome have been identified and characterized (Nazerian et al., 1991; van den Hurk, 1992; Zhang et al., 1991). Recently, the predicted sialidase was found to be part of the TAdV-3 virion structure, in addition to a 13.32 kDa-novel polypeptide of yet unknown function (Kumar et al., 2015). Whether the rest of the predicted genes/ORFs are expressed and translated is yet to be unveiled.

TAdV-3 is, by far, the most extensively studied siadenovirus in the context of virus morphology, structure, pathobiology, vaccine development, and genomic characterization. Nevertheless, some aspects of the virus life cycle have yet to be investigated. Among these aspects are a detailed growth kinetics in host cells and the accompanying gene expression patterns during active infection. The goals of the current study were to (1) demonstrate the different phases of the TAdV-3 replication cycle in host cells using in-house qPCR-based virus infectivity assay, and (2) verify and define the complete mRNA transcription patterns of the 23 TAdV-3 genes/ORFs during the first 24 h of the replication cycle. By achieving these goals, we can gain a better understanding of the TAdV-3 life cycle, which can further the field of siadenoviral biology.

2. Materials and methods

2.1. Virus and cell culture

A commercially available HE cell culture vaccine product was used as a source for avirulent TAdV-3. Stock virus was titrated following the qPCR-based infectivity assay developed in our laboratory (Mahsoub et al., 2017), where the titer was expressed as infectious viral particles (IVPs)/mL. Small aliquots of virus inoculum were stored at −20 °C and used as needed. MDTC-RP19 cells (RP19; a lymphoblastoid turkey cell line) were purchased from the American Type Culture Collection (Manassas, VA) and used for virus propagation and infection experiments. Cells were grown in suspension cultures at 41 °C in a humid environment containing 5% CO_2, using 1:1 Leibovitz L-15/McCoy's 5 A medium supplemented with 10% fetal bovine serum (FBS), 20% chicken serum (ChS), 5% tryptose phosphate broth (TPB), and 1% antibiotics solution (10,000 units/mL of penicillin, 10,000 µg/mL of streptomycin). When infected, RP19 cells were maintained in serum-reduced media (SRLM) composed of 1:1 Leibovitz L-15/McCoy's 5 A medium supplemented with 2.5% FBS, 5% ChS, 1.2% TPB, and 1% antibiotics solution.

2.2. Growth curve

RP19 cells (5×10^5 cells/mL) were inoculated with TAdV-3 at a multiplicity of infection (m.o.i.) of 20 IVPs/cell. After adsorption for 1 h at 41 °C, the cells were washed three times with SRLM by centrifugation at 3000 r.p.m. and final resuspension in SRLM. One mL of inoculated cells was added to each well in 24-well cell culture plates, and incubated at 41 °C. Well contents (~1 mL) were collected at 1, 6, 12, 18, 24, 36, 48, 60, 72, 96, 120, and 168 h.p.i. and frozen at −20 °C until used later for virus titration. Prior to titration, samples were lysed by three successive freeze-thaws and infectious titers were determined following the qPCR method (Mahsoub et al., 2017), with modifications. Briefly, in 1.5-mL microcentrifuge tubes, 0.5 mL of SRLM containing 5×10^5 RP19 cells were added and inoculated with 100 µL of the samples harvested at the indicated time points above. The inoculated cells were incubated at 41 °C for 1 h and then pelleted at 3000 r.p.m. for 7 min at 4 °C. Cells were then washed three times with SRLM to remove unattached virus particles and free viral DNA. Cell pellets were re-suspended in 200 µL of phosphate-buffered saline (PBS) and stored at −20 °C until DNA extraction using QIAamp DNA mini kit (Qiagen, Valencia, CA). DNA was eluted in 50 µL of DNase/RNase-free water and qPCR was performed with 1 µL DNA per reaction to determine the number of IVPs.

2.3. Detection of newly synthesized viral DNA by Southern blot analysis

The time course for DNA synthesis was determined as described by Alexander et al. (1998), with some modifications. RP19 cells (1×10^6/mL) were grown in T-75 cell culture flasks and inoculated at an m.o.i. of 20 IVP. Inoculated cells from an entire flask were harvested at the following time points: 2, 4, 6, 8, 10, 12, 18, and 24 h.p.i. Cells from non-infected flask was used as a negative control. Cells were centrifuged at 3000 r.p.m., washed in PBS, pelleted in 1.5-mL Eppendorf microcentrifuge tubes, and frozen at −70 °C. Cell pellets were thawed, 30 µL of 0.4 M NaOH were added, tubes vortexed, followed by incubation at 80 °C for 10 min. Dot blotting on Zeta-Probe™ membranes (Bio-Rad, Hercules, CA) was performed. The membrane was soaked in warm, distilled water and briefly washed in 0.4 M NaOH. For each time point, 30 µL of purified DNA were loaded on the membrane. DNA from uninfected cells served as a negative control. The membrane was rinsed with 100 mL of 0.4 M NaOH after the samples were fully loaded and washed twice in 2 × saline sodium citrate (SSC) buffer (1 × SSC buffer contains 150 mM NaCl and 15 mM sodium citrate in molecular biology grade water, pH 7.0) for 5 min. The membrane was then air-dried and crosslinked using a UV crosslinker (Fisher Scientific, Hampton, NH) at λ = 1200 nm. The membrane was pre-hybridized at 68 °C for 5 h in a hybridization oven (UVP HB-1000 Hybridizer) in 20 mL of hybridization solution (5 × SSC, 0.1% N-lauroylsarcosine, and 0.02% sodium dodecyl sulphate [SDS]) with 1% blocking reagent (Roche, Sigma-Aldrich, St. Louis, MO). The blocking agent was removed and replaced with hybridization solution containing 0.5% blocking reagent and 5 mL of freshly denatured probe. The probe was a 500-bp TAdV-3 hexon gene fragment. The fragment was labelled using the DIG DNA Labeling Kit (Roche, Sigma-Aldrich, St. Louis, MO) according to the manufacturer's instructions. Hybridization was carried out at 68 °C overnight followed by two 5-min washes in 2 × SSC, 0.1% SDS at room temperature and two washes at 68 °C in 0.1 × SSC, 0.1% SDS for 15 min. The membrane was developed using the DIG DNA Detection Kit (Roche, Sigma-Aldrich, St. Louis, MO) according to the manufacturer's instructions.

2.4. Total RNA extraction from TAdV-3-infected RP19 cells

Ten mL of RP19 cells at 1×10^6 cells/mL were inoculated with TAdV-3 at an m.o.i. of 20 IVP in T-25 cell culture flasks and incubated for 1 h at 41 °C. Cells were then washed 3 times to remove unattached virus, resuspended in 10 mL of SRLM, transferred to new T-25 flasks, and incubated at 41 °C. At different time points post-adsorption (*i.e.*, 2, 4, 8, 12, 18, and 24 h), the 10 mL of inoculated cultures (*i.e.*, 1×10^7 cells total) were collected from each T-25 flask in 15-mL conical centrifuge tubes, and pelleted at 1200 r.p.m. for 7 min at 4 °C. Total RNA was extracted from cell pellets using TRIzol™ Reagent (Life

Technologies, Thermo Fisher Scientific, Carlsbad, CA) according to the manufacturer's instructions. To remove residual genomic DNA, extracted RNA was incubated with DNase I (Qiagen, Valencia, CA) for 30 min at room temperature. Residual DNase I was then removed by using RNeasy spin columns (Qiagen, Valencia, CA). The purified RNA samples were immediately stored at −80 °C until used for cDNA synthesis. RNA was quantified by reading the absorbance at λ = 260 nm on a NanoDrop spectrophotometer (Fisher Scientific, Hampton, NH). Total RNA integrity was verified on a denaturing gel composed of 2.5% agarose containing 6% (w/v) formaldehyde, 20 mM 3-(N-morpholino)propanesulfonic acid (MOPS buffer, pH 7.0) and 1 mM ethylenediaminetetraacetic acid (EDTA) with running buffer composed of 20 mM MOPS (pH 7.0) and 1 mM EDTA. The gel was pre-run at 100 V for 10 min, total RNA samples were then loaded, and the run was continued at 100 V until the bromophenol blue dye migrated at least 2/3 of the gel length. The gel was visualized on a UV transilluminator.

2.5. RT-PCR (reverse transcriptase-polymerase chain reaction) for detection of TAdV-3 transcripts

Culture samples from the growth curve experiment were used for RNA extraction to study the gene expression kinetics of TAdV-3. First-strand complementary DNA (cDNA) was synthesized with total RNA from each time point using Thermoscript™ Reverse Transcriptase (RT) kit (Invitrogen, Life Technology, Grand Island, NY), according to the manufacturer's instructions. The kit included avian myeloblastosis virus (AMV) reverse transcriptase with reduced RNase H activity. First, in 0.2-mL Eppendorf Mastercycler™ PCR tubes 12-μL reactions consisting of 1 μg of total RNA, 1 μL of 50 mM oligo(dT) primer, and 2 μL of 10 mM dNTP Mix were mixed. Reactions were incubated at 65 °C for 5 min for RNA denaturation, followed by a 2-min incubation on ice. Second, an 8-μL mastermix consisting of 4 μL of 5 × cDNA synthesis buffer, 1 μL of 0.1 M DTT (dithiothreitol), 1 μL of RNaseOUT™ (ribonuclease inhibitor; 40 U/μL), 1 μL of DEPC-treated water, and 1 μL of ThermoScript™ RT (15 units/μL) was added to each reaction in PCR tubes. The 20-μL reactions were incubated for 60 min at 55 °C for cDNA synthesis and heated at 85 °C for 5 min for reaction termination. Two microliters of RNase H were then added to each reaction and incubated at 37 °C for 20 min to remove RNA templates. A second set of reactions was prepared in parallel, but without adding the reverse transcriptase. Products served as negative RT-PCR controls and to verify the efficient removal of viral DNA by the DNase treatment during RNA extraction step. cDNA products were stored at −20 °C until used later in PCR amplification. cDNA was diluted at 1:10 in DEPC-treated water and 2 μL were added to 23 μL of the PCR mixture. A final PCR volume of 25 μL was made, containing 1 × PCR buffer, 1.5 mM $MgCl_2$, 25 pmol of each primer, 200 nM dNTP mix, and 0.5 IU of platinum *Taq* polymerase (Invitrogen, Life Technology). The PCR amplification conditions were 2 min at 94 °C for initial denaturation and enzyme activation, followed by 35 cycles of 30 s at 94 °C for denaturing, 30 s at 55 °C for annealing, and 1 min at 68 °C for extension. Nucleotide sequences and features of primers are listed in Table 1. All primers were 20–22 nucleotides and specific for each ORF with GC content of 40–60% and melting temperatures of 50–60 °C. Primers were designed using Primer3 Plus™ based on the published nucleotide sequence of TAdV-3 VAS genome [GenBank accession: AY849321.1; (Beach et al., 2009)] and analyzed with BLAST to ensure their specificity to the genes/ORFs of interest. To verify the amplification of target fragments and therefore the expression of target genes, PCR products from each primer set were analyzed by 1–2% agarose gel electrophoresis (100 V for 45–60 min) and visualized by ethidium bromide staining. Equal amounts of PCR products from the 6 time points studied for each gene (*i.e.*, 25 μL of prepared PCR sample) were loaded and analyzed on the same gel. This allowed for a relatively accurate comparison of gene expression at different time points based on the cDNA band intensity.

3. Results

3.1. Avirulent TAdV-3 growth kinetics and DNA synthesis in RP19 cells

The growth curve of avirulent TAdV-3 in RP19 cells infected at an m.o.i. of 20 IVP is displayed in Fig. 1A. A sigmoid-like growth curve featuring lag, log, and decline phases of virus infectious titer was obtained. The initial lag/decline phase lasted for 18 h.p.i., in which the infectious virus titer dropped during the first 12 h and became steady till 18 h.p.i. The log phase then followed and continued from 18 to 120 h.p.i., in which the virus grew exponentially and reached peak titers of 3.42×10^8/0.1 mL. During this phase, which lasted more than 4 days, the infectious virus titer increased by 20,834 folds. After that, a short phase of slight decline in virus titer was observed at day 6 p.i. In this experiment, virus cytopathic effect (CPE) manifested by cell enlargement was observed by 72 h.p.i., where the titer was 8.36×10^6/0.1 mL, *i.e.*, 509 times of that at 18 h.p.i.

The synthesis of nascent viral DNA within RP19 cells was studied by running a time course infection experiment. Samples from infected culture were collected every 2 h between 2 and 24 h.p.i. and Southern blot analysis was performed to detect newly synthesized viral DNA. The initiation of viral DNA replication was pinpointed to 8 h.p.i. as indicated by the higher intensity of the viral DNA spot at this time point as compared to the earlier time points. Viral DNA was detected at similarly high levels thereafter (Fig. 1B).

3.2. Transcriptional kinetics of TAdV-3 genes/ORFs in RP19 cells

To study the temporal expression of TAdV-3 mRNA, total RNA was extracted from TAdV-3-infected RP19 cells at sequential time points post-infection (p.i.) and reverse-transcribed with oligo(dT) primer. Aliquots of cDNA synthesized at each time point were used for the gene-specific PCR and therefore transcriptional analysis of the 23 TAdV-3 genes/ORFs identified previously (Beach et al., 2009). Although quantitative RT-PCR was not perfumed, our strategy for standard RT-PCR and gel analysis allowed for reliable evaluation of the relative abundance of specific mRNAs from individual genes/ORFs at the different time points. Before using total RNA in RT-PCR, its integrity was verified on a denaturing (formaldehyde) agarose gel. The 28S rRNA band appeared at 4.5 kb and the 18S rRNA band appeared at 1.9 kb. The intensity of the 28S band was as twice as that of the 18S band. Total DNase I-treated mRNA appeared as a smear from 0.5 to 12 kb, while rRNA bands were clear and sharp (Fig. 2C). TAdV-3 genes/ORFs listed in Table 2 are organized from left to right with the upper (or right) and lower (or left) strands of the virus genome indicated with *r* and *l*, respectively. Nucleotide positions and gene/ORF names corresponding to those of the VAS of TAdV-3 were used. The E1, E3, and E4 transcription units are so designated merely on the basis of their location as compared with other adenoviral genera. Nucleotide sequences in these regions are exclusive to the genus *Siadenovirus* and share no homology with other adenovirus members (Beach et al., 2009; Kovács and Benkő, 2011; Pitcovski et al., 1998). The expression patterns and accumulation of the individual TAdV-3 gene transcripts *in vitro* over a 24-h time course post-infection are displayed in Table 2 and Fig. 2A, respectively. To verify the absence of viral DNA contamination in RNA extracts, no-reverse transcriptase RT-PCR reactions were performed with hexon-specific primers. No amplification was observed with any RNA from the time points studied (Fig. 2B). This process guaranteed that the amplified RT-PCR products genuinely represent the virus-expressed mRNAs.

The TAdV-3 E1 region is located on the left terminus of the *r* strand of the TAdV-3 genome. From the TAdV-3 E1 transcription unit, two transcripts from the sialidase (ORF1) and hyd ORFs were detected by RT-PCR. ORF1 mRNA was first detected at 4 h.p.i., while hyd mRNA was first detected at 2 h.p.i; and both increased gradually throughout the early and late phases of TAdV-3 transcription until reached maximum levels at 24 h.p.i. The TAdV-3 E2B transcription unit, located on

Table 1
Oligonucleotide primer pairs used with RT-PCR for the analysis of TAdV-3 gene expression.

Primer name	Gene coordinates[a]	Nucleotide sequence (5′-3′)	Primer starting position[b]	Tm[c]	Amplicon size
TAdV-3-ORF1_F	313-1953	CTGTGCGTTACCCTCTCCAT	131	60.1 °C	567 bp
TAdV-3-ORF1_R		TCCACGAAACACAAGGAACA	697	60.1 °C	
TAdV-3-hyd_F	2098-2325	TGCGTTACTATCCTGGCACA	4	60.3 °C	184 bp
TAdV-3-hyd_R		AAAAGTCTCGGCACAGCAAC	184	60.4 °C	
TAdV-3-IVa2_F	2334-3437	TCCCTCGAGTATTGCTGACC	148	60.2 °C	641 bp
TAdV-3-IVa2_R		TACAACCAATGCCAGAAACG	641	59.6 °C	
TAdV-3-AdPol_F	3430-6768	AAGGCTCTTGTCCACGCTAA	659	60.0 °C	562 bp
TAdV-3-AdPol_R		CGTGGAACACTTGCTGCTTA	1220	60.0 °C	
TAdV-3-pTP_F	6765-10995	ATTTCAGGCTGCCATTTGTC	983	60.1 °C	576 bp
TAdV-3-pTP_R		TCATTTGCTGATTGGCTACG	1558	59.8 °C	
TAdV-3-52 K_F	8570-9472	GCTAGATGGGGATCAAAAGC	225	58.7 °C	611 bp
TAdV-3-52 K_R		TTCCAGGCTGATCTGCATAA	835	59.4 °C	
TAdV-3-pIIIa_F	9462-10979	ATACCGTTGCTCCTCCAATG	731	60.0 °C	576 bp
TAdV-3-pIIIa_R		CTGTTTTTGAAGGCCTGGAC	1306	59.7 °C	
TAdV-3-III_F	11001-12347	AATTTTTGCTCCAACGGAAG	27	59.2 °C	593 bp
TAdV-3-III_R		CAATAGCCCAACCAGGAAGA	619	60.1 °C	
TAdV-3-pVII_F	12347-12709	ATTTGATAGGTGGCGCTTTG	74	60.1 °C	213 bp
TAdV-3-pVII_R		GTACAGGAACTGCAGGCACA	286	59.9 °C	
TAdV-3-pX_F	12712-12888	GCACCCAGAAAAGGTCTAAAAA	16	59.6 °C	145 bp
TAdV-3-pX_R		CTGCAATTACAGTTCCAGCAA	160	59.0 °C	
TAdV-3-pVI_F	12906-13601	GGCAGGATTAGCAGGTCAAA	234	60.2 °C	303 bp
TAdV-3-pVI_R		GACAAAGCAGGGGTGTCAAT	536	60.0 °C	
TAdV-3-II_F	13610-16330	ATGAAGAGGGTCCTCCAGGT	1079	59.9 °C	544 bp
TAdV-3-II_R		GGATCTTTCCTGAACCACCA	1622	59.9 °C	
TAdV-3-EP_F	16332-16976	AGTGTCCTTGTTCTGCTGCAT	341	59.9 °C	301 bp
TAdV-3-EP_R		CGCGCAAATAAAAACAATACA	641	58.8 °C	
TAdV-3-DBP_F	16973-18186	TTGCAGATTTGTCTGCCAAG	377	60.0 °C	588 bp
TAdV-3-DBP_R		GGCCAAACTGGTTGAGACAT	964	60.0 °C	
TAdV-3-100 K_F	18230-20227	TAGACTCTGCAGCGCAAGAA	23	60.0 °C	506 bp
TAdV-3-100 K_R		TGGCAGAGAATCTGTTGCTG	528	60.1 °C	
TAdV-3-33 K_F	20142-20699	CGAGCCCATACATGAAGGAA	2	61.0 °C	217 bp
TAdV-3-33 K_R		TTGTAAAGCCTTAGCATCCAA	218	57.6 °C	
TAdV-3-22 K_F	20142-20411	GTTTCACAGCCCAGAAGAGG	12	59.8 °C	186 bp
TAdV-3-22 K_R		GGAATTTGTATGCCCTTTGC	197	59.4 °C	
TAdV-3-pVIII_F	20769-21371	AAGATGAACCTGCCCAGTTG	218	60.1 °C	308 bp
TAdV-3-pVIII_R		GCTAATAGCACCTCCGGTGA	525	60.2 °C	
TAdV-3-E3_F	21247-22116	CGGAGGTGCTATTAGCCTCA	32	60.4 °C	410 bp
TAdV-3-E3_R		CAATGGGTAAGCCCCATCTA	441	59.8 °C	
TAdV-3-U exon_F	22260-22520	TTGATGGGAAGAGAGTTTCCA	24	59.7 °C	214 bp
TAdV-3-U exon_R		TGTTCCTGTTGCAAACCAAG	237	59.7 °C	
TAdV-3-IV_F	22519-23883	TTGAAGCAACACCTCCCTTT	122	59.7 °C	594 bp
TAdV-3-IV_R		GCAATGCTAATCCTCCTGCT	715	59.4 °C	
TAdV-3-ORF7_F	24512-25168	CAAGCAATGGCTGAGAACAA	82	60.0 °C	377 bp
TAdV-3-ORF7_R		ACCAGCAACACGAGAGGTTT	458	59.8 °C	
TAdV-3-ORF8_F	25204-25701	AGCACACCACGCAAGTACAC	94	59.8 °C	308 bp
TAdV-3-ORF8_R		CGATGCCTACACCATCATCA	401	60.5 °C	

[a] Relative to the 26,266 bp genome size.
[b] Relative to the gene size.
[c] Tm, primer melting temperature.

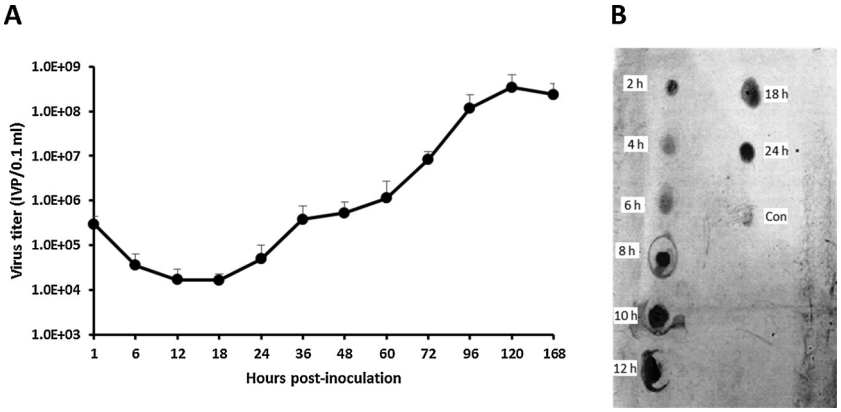

Fig. 1. (A) One-step growth curve for avirulent turkey adenovirus 3 (TAdV-3) in RP19 cells. Cells were inoculated with virus at an m.o.i. of 20 IVP. Total virus titer was determined by qPCR-based infectivity assay at the intervals indicated. Data shown are from experiments performed in triplicate, with error bars indicating standard deviations. The virus infectious titer began to increase at 18 h.p.i. IVP, infectious viral particle. (B) Southern blot for the specific detection of new viral DNA synthesis in infected RP19 cells. Lysates of infected cells were collected at 2 h intervals, *i.e.*, 2–24 h.p.i.; control-uninfected RP19 cell lysate (Con) was also included. Significant increase in viral DNA can be seen starting from 8 h.p.i.

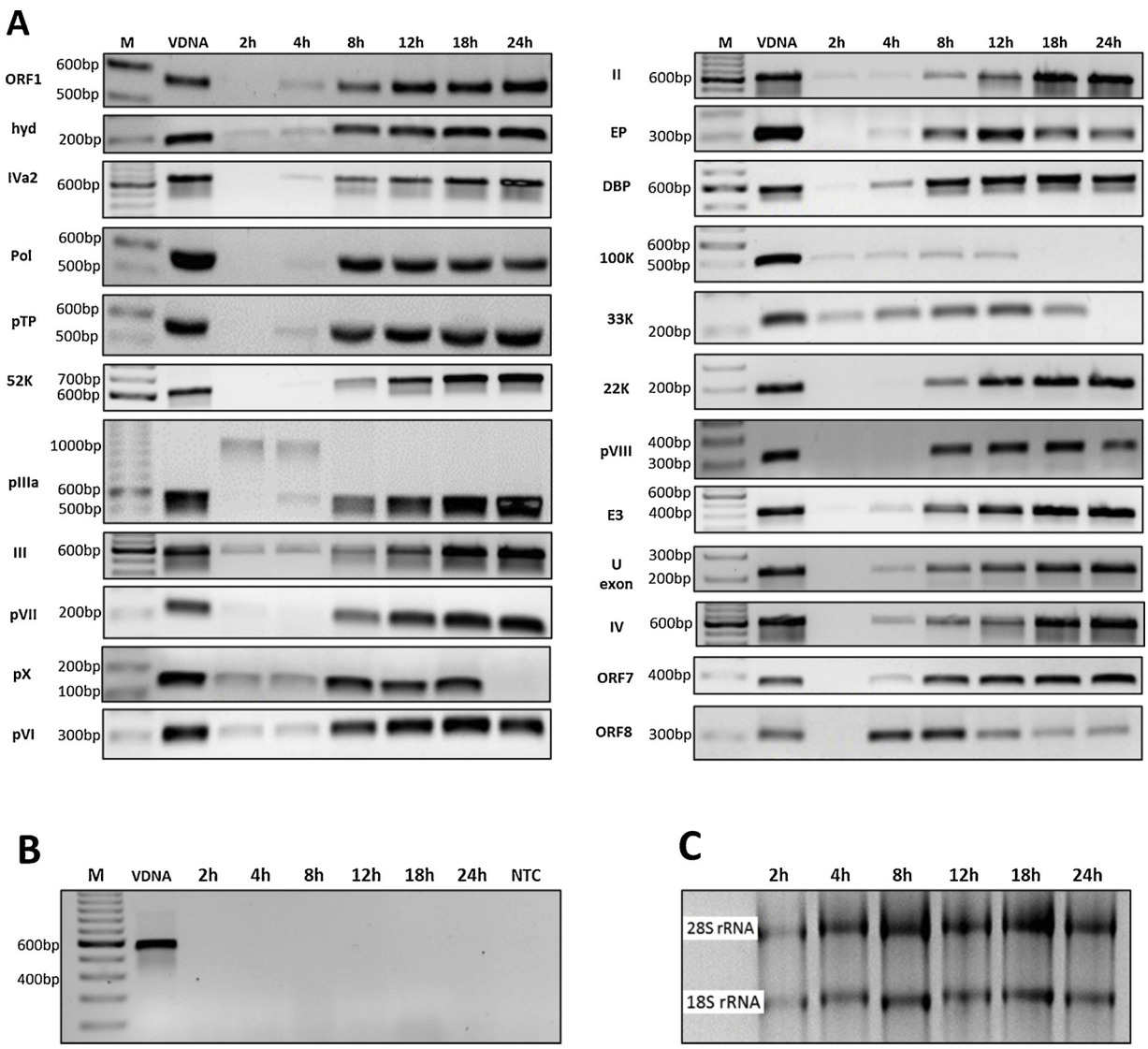

Fig. 2. (A) Expression and accumulation of the 23 TAdV-3 gene transcripts over a period of 24 h post-infection as studied by RT-PCR and agarose gel analysis. (B) Negative RT-PCR reactions were performed on non-RT cDNA products using primers specific to hexon gene. In (A) and (B) The amount of RT-PCR sample applied in each lane was 25 µL per well. M, 100-bp DNA molecular weight marker; VDNA, viral DNA used as a positive PCR control (lane 2). (C) Denaturing gel analysis confirmed the integrity of total RNA extracted from virus-infected RP19 cells at different time points p.i. Three µL per well were loaded.

the *l* strand, contains three genes coding for IVa2, pol, and pTP proteins. IVa2 mRNA was first detected at 4 h.p.i. at a low level and its expression increased gradually thereafter. The expression of pol transcript was first detected at 4 h.p.i. at a very low level, increased sharply at 8 h.p.i. to the highest level, and then decreased slightly throughout the late phase of the virus replication cycle. Like pol, pTP mRNA was expressed at a very low level at 4 h.p.i., increased sharply at 8 h.p.i., but continued to slightly increase thereafter until reaching its highest level at 24 h.p.i. TAdV-3 E2 A transcription unit is located on the *l* strand of the TAdV-3 genome and contains one gene coding for the DBP protein. DBP mRNA was expressed at a moderate level at 4 h.p.i. Thereafter, its expression increased sharply, reaching its maximum level at 18 h.p.i., then declined marginally at 24 h.p.i. TAdV-3 E3 region is located on the *r* strand of the TAdV-3 genome within the major late transcription unit and encodes only the putative E3 ORF. E3 transcript was first detected at a low level at 4 h.p.i. and continued to be detected at increasing levels until reached the highest at 18–24 h.p.i. TAdV-3 E4 region is located on the right terminus of the TAdV-3 genome and encodes two ORFs: one is found on the *r* strand, ORF7; while the other is found on the *l* strand, ORF8. Transcripts of ORF7 and ORF8 were first detected at 4 h.p.i. and continued throughout the early and late phases of TAdV-3 replication. Interestingly, the two ORFs showed completely opposite expression patterns, *i.e.*, ORF7 mRNA started at a minimum level at 4 h.p.i. and increased gradually till reaching a maximum at 24 h.p.i., while ORF8 mRNA level was the highest at 4 h.p.i. and declined detectably till reaching the lowest level at 24 h.p.i. The ORF8 expression pattern is unique among all TAdV-3 genes.

Fourteen ORFs/genes have been mapped to the TAdV-3 major late transcription unit (Beach et al., 2009): 52 K, pIIIa, III, pVII, pX, pVI, hexon, protease, 100 K, 22 K, 33 K, pVIII, fiber, and U exon; all of which are located on the *r* strand, except for the U exon. RT-PCR analysis (Table 2 and Fig. 2A) revealed various transcriptional patterns and transcription start times for the different late genes The expression of 52 K was detected at a very low level at 8 h.p.i. and increased gradually thereafter until reached a maximum level at 24 h.p.i. RT-PCR amplification of pIIIa revealed the presence of two transcripts specific to this gene; at low expression levels the large transcript was detected at 2 h.p.i and both transcripts were co-detected at 4 h.p.i.; only the small (permanent) transcript was increasingly detectable from 8 till 24 h.p.i. For the major capsid protein genes, hexon and penton mRNAs were

Table 2
Temporal expression patterns of TAdV-3 genes in RP19 cells as determined by RT-PCR.

ORF, strand[a]	Transcription unit[b]	*In vitro* expression of TAdV-3 at different time points					
		2 h	4 h	8 h	12 h	18 h	24 h
ORF1, *r*	E1	–	+	+	+	+	+
hyd, *r*	E1	+	+	+	+	+	+
IVa2, *l*	E2B	–	+	+	+	+	+
Pol, *l*	E2B	–	+	+	+	+	+
pTP, *l*	E2B	–	+	+	+	+	+
52 K, *r*	ML	–	–	+	+	+	+
pIIIa, *r*	ML	–	+	+	+	+	+
III (penton), *r*	ML	+	+	+	+	+	+
pVII, *r*	ML	–	–	+	+	+	+
pX, *r*	ML	+	+	+	+	+	–
pVI, *r*	ML	+	+	+	+	+	+
II (hexon), *r*	ML	+	+	+	+	+	+
EP, *r*	ML	–	+	+	+	+	+
DBP, *l*	E2 A	–	+	+	+	+	+
100 K, *r*	ML	+	+	+	+	–	–
33 K, *r*	ML	+	+	+	+	+	–
22 K, *r*	ML	–	–	+	+	+	+
pVIII, *r*	ML	–	–	+	+	+	+
E3, *r*	E3	–	+	+	+	+	+
U exon, *l*	L	–	+	+	+	+	+
IV (fiber), *r*	ML	–	+	+	+	+	+
ORF7, *r*	E4	–	+	+	+	+	+
ORF8, *l*	E4	–	+	+	+	+	+

[a] hyd, hydrophobic protein; pTP, terminal protein precursor; EP, endoprotease; DBP, DNA binding protein; *r* = right or upper strand; *l* = left or lower strand.

[b] The assignment of E2 A, E2B, and ML transcription units is based on homology with members of the family *Adenoviridae*; however, the assignment of E1, E3, and E4 transcription units is based on their location only; L, late.

detected at low levels starting at 2 h.p.i., while fiber mRNA was first detected at 4 h.p.i. at low level, too. The amount of transcripts from the three genes steadily increased throughout the late phase of infection. The expression of pVII transcripts was first detected at 8 h.p.i. and gradually increased throughout the late phase of infection. pX mRNA was detected at low level at 2 and 4 h.p.i., increased between 8 and 18 h.p.i., but was not observed thereafter. The expressions of pVI was detected at very low levels at 2 and 4 h.p.i., increased gradually until reached a maximum level at 18 h.p.i., and slightly declined by 24 h.p.i. EP mRNA was first detected at 4 h.p.i. at a low level, reached a maximum level at 12 h.p.i., and continued to be detected at lower levels throughout the late phase of TAdV-3 gene expression. The expression of 100 K transcript was very low at 2 h.p.i. and continued to be detected at low levels till 12 h.p.i., after which it was not observed. The transcript of 33 K gene was detected as early as 2 h.p.i., increased detectably till reached a maximum level at 12 h.p.i., reduced in level at 18 h.p.i., and vanished by 24 h.p.i. The expression of 22 K mRNA began to be detectable at 8 h.p.i. and continued to increase throughout the late phase of infection. pVIII mRNA was first detected at 8 h.p.i. and continued to be detected at high levels till 18 h.p.i., after which the level was relatively low. The U exon transcript showed a transcriptional pattern very similar to E3, where it was detected at 4 h.p.i. for the first time, and increased gradually till reached a maximum at 24 h.p.i.

4. Discussion

4.1. TAdV-3 life cycle

In this study, we report for the first time the several aspects of TAdV-3 life cycle *in vitro*, including the start of genome replication, the phases of virus productive cycle, and a complete profiling of viral gene expression. Active virus replication is often verified and analyzed by growth curves, in which viral multiplication in the presence of host cells is measured as a function of time (Dulbecco and Vogt, 1954). Since there is only one established cell line that is susceptible to TAdV-3 infection, *i.e.*, RP19 cells, which grows in suspension culture, there were limited options to accurately study the virus growth kinetics *in vitro*. Previous studies have investigated some aspects of TAdV-3 infection and replication *in vitro* by either determining the number of infected cells -primary leukocytes- by immunofluorescence (van den Hurk, 1990) or detecting the virions using electron microscopy (Nazerian and Fadly, 1982). Using our in-house qPCR-based infectivity assay (Mahsoub et al., 2017) to determine virus infectious titers, we were able to study the growth kinetics of TAdV-3 in cultures of RP19 cells.

TAdV-3 growth curve started with a lag phase during which the number of infectious viral particles was declined, indicating the successful internalization of virus particles. After receptor-mediated endocytosis, adenoviruses undergo a cascade of subcellular events ending with virion disassembly before reaching the nuclear pore. Consequently, internalized virus particles lose essential structural components and become non-infectious (Henaff et al., 2011). The replication of TAdV-3 genome started at approximately 8 h.p.i. as detected by Southern blot analysis and continued for at least 24 h.p.i. (Fig. 1B); this was consistent with our finding regarding the early/intermediate expression of the 3 major genes involved in DNA replication, *i.e.*, pTP, DBP, and pol. Replication of adenovirus genome can take up to 8 h post-infection, followed by a rapid (4–6 h) late phase ending with the assembly of new virus particles (Russell, 2000). According to the described timeline, progeny adenovirus can be produced after 12–14 h of successful infection. However, due to the considerable variations among adenovirus species in terms of the genetic organization and the complexity of virus-host process (Chardonnet and Dales, 1970a, b; Davison et al., 2003), the time required for the complete productive cycle may vary significantly. Following the lag phase, the generation of new TAdV-3 progeny was first detected between 18 and 24 h.p.i. (Fig. 1A). This result is in accordance with previous electron microscopy studies which detected TAdV-3 virions in the nuclei of infected turkey leukocytes at 18–24 h.p.i. (van den Hurk, 1990). By 8 h.p.i. all TAdV-3 early and late genes have been expressed, which suggests that it took a period of 10 h from the initiation of gene transcription till the assembly of mature virions. During this interval, a series of events occur involving early-late gene expression switch, posttranscriptional and posttranslational modifications, DNA encapsidation, and eventually virus release (Berk, 2007). The exponential phase of TAdV-3 growth continued thereafter and reached its peak by 120 h.p.i. Using light microscopy, CPE in TAdV-3-infected RP19 cultures was observed by 72 h.p.i. Enlargement and ballooning of infected lymphocytes is a typical CPE of TAdV-3 infection due to the accumulation of progeny virus in the nucleus (Nazerian and Fadly, 1982). Previous studies reported the development of CPE at 36 h.p.i. in RP19 cells infected at an m.o.i. of 50 IVP (Mahsoub, 2015).

4.2. TAdV-3 gene expression profile

Although the nucleotide sequence, genome organization, and detailed transcriptional maps (based on cDNA sequencing) have been achieved for a number of adenovirus species (Biasiotto and Akusjarvi, 2015; Wu et al., 2013), the mRNA expression pattern of the individual adenoviral genes during the virus infectious cycle have not been adequately investigated. Determining the viral gene expression pattern should provide more insight into the strategies and mechanisms of virus replication. Annotation of TAdV-3 genome and the assignment of genes were merely based on bioinformatic analysis and comparisons with data from other adenovirus species. Putative ORFs with no sequence homology with genes of known functions have been detected (Beach et al., 2009; Pitcovski et al., 1998). The present study provides essential information about the expression of the predicted TAdV-3 ORFs that share no homology with other genes as well as of the established genes,

shared with other adenoviruses. This is the first report about the gene expression analysis in genus *Siadenovirus*. Under the current investigation, single mRNA products were detected for the TAdV-3 genes/ORFs, except for the early pIIIa gene which had two mRNAs, one temporary and one permanent. RT-PCR analysis of fowl adenovirus genes showed the presence of more than one transcript from several late genes: penton, pVII, pX, 100 K, and fiber (Ojkic et al., 2002).

Using specific RT-PCR assays, we detected mRNA products from the 23 TAdV-3 ORFs/genes and identified their temporal expression patterns. Overall, 7 genes started expression at 2 h.p.i., 12 genes started at 4 h.p.i., and only 4 genes started expression as late as 8 h.p.i. All gene transcripts continued to be detected throughout the late phase of virus transcription, except for 3 genes that were last detected at 12 h.p.i. (*i.e.*, 100 K) and 18 h.p.i. (*i.e.*, pX and 33 K). Some early expressed adenoviral genes are involved in viral DNA replication and the regulation of transcription levels (Fessler and Young, 1998; Shu et al., 1988). Comparing TAdV-3 transcriptional kinetics with those reported for avian, porcine, and human adenoviruses (Akusjarvi, 2008; Biasiotto and Akusjarvi, 2015; Cao et al., 1998; Ojkic et al., 2002; Payet et al., 1998; Reddy et al., 1998) suggests the existence of considerable variations in the regulation of gene expression among the various adenoviral genera. In this context, the transcriptional kinetics of genus *Siadenovirus* may be unique since it has the shortest genome in the family.

The 22 K protein was reported to have several roles in the replication of mammalian adenoviruses. These roles include DNA packaging; virion assembly; early-to-late phase switch of gene transcription, *i.e.*, activation of MLP; stimulating the expression of V protein, penton base, and adenovirus death protein; stimulating the accumulation of hexon protein; and controlling the 33 K accumulation. Since the roles of the 22 K and 33 K seem to be overlapping and/or interchangeable (Ahi and Mittal, 2016; Biasiotto and Akusjarvi, 2015), the expression pattern of TAdV-3 22 K compared with that of 33 K suggests that the former plays a more important role in TAdV-3 replication. The TAdV-3 33 K protein gene is increasingly expressed from 2 h.p.i. to 18 h.p.i. Some roles of the TAdV-3 33 K protein might be compensated by the 22 K protein and other regulatory elements. Since the expression of TAdV-3 22 K gene starts at 8 h.p.i. and we observed changes in the transcription levels of some genes between 4 and 12 h.p.i., it is tempting to suggest a role for the 22 K protein in controlling the transcription patterns of some TAdV-3 genes. However, these notions will need to be experimentally investigated. TAdV-3 lacks several proteins found in mammalian adenoviruses, with which the 22 K protein interacts.

All members of family *Adenoviridae* share similar genetic organization in the central portion of the genome. Extensive variations that distinguish the different adenoviral genera are found in the terminal regions, which largely code for the early proteins (Davison et al., 2003). Although minimal or no sequence homology exists in these regions among the recognized genera, similar terminology was used to identify them based on their location in the respective genomes. Unique to the genus *Siadenovirus* are E1 ORF1 and hyd; E3 ORF; and E4 ORF7 and ORF8. The expression patterns of these ORFs suggest critical roles of their putative proteins in the TAdV-3 life cycle. Future research endeavors should aim to discover the roles of these proteins. Interestingly, sialidase, a once-putative ORF1 product, has recently been verified as a structural component in the TAdV-3 virion (Kumar et al., 2015). The potential function of this sialidase in the TAdV-3 infectious cycle needs further investigation. Another hypothetical structural protein (*i.e.*, TaV3gp04) of 13.32 kDa has also been identified (Kumar et al., 2015). This protein was suggested to be a product of a hypothetical E1-ORF4 mapped to TAdV-3 genome by Pitcovski et al. (1998), but not by Beach et al. (2009). Since our RT-PCR assays were based on the nucleotide sequence of TAdV-3 ORFs identified by Beach et al. (2009), the expression of ORF4 was not investigated in this study. ORF4 has been also mapped to the E1 region of the raptor siadenovirus 1 genome (Kovács and Benkő, 2011); and thus considered a conserved ORF within the genus *Siadenovirus*. Transcriptional analysis of ORF4 will be considered in our future research on TAdV-3.

The expression of the U exon was detected beginning 4 h.p.i. and continued to increase thereafter. This exon is present in the majority of adenovirus genera and is regulated by a minor late promoter (Davison et al., 2003); however, whether a functional protein is expressed from it is yet to be known. The structure and function of capsid and core structural proteins of adenoviruses in general and TAdV-3 in particular have been extensively characterized (Nazerian et al., 1991; Russell, 2009; van den Hurk, 1992; Zhang et al., 1991).

In conclusion, this study provides information about the replication and transcriptional kinetics of TAdV-3-A in host B lymphocytes. Further studies aiming at delineating the transcriptional map of TAdV-3 genome are underway.

Acknowledgments

This work was supported by Cargill, Inc (Harrisonburg, VA, USA), Virginia Poultry Growers Cooperative, LLC. (Hinton, VA, USA), and the Egyptian Ministry of Higher Education and Scientific Research (Cairo, Egypt).

References

Adams, M.J., Lefkowitz, E.J., King, A.M.Q., Carstens, E.B., 2014. Ratification vote on taxonomic proposals to the International Committee on Taxonomy of Viruses (2014). Arch. Virol. 1–11.
Ahi, Y.S., Mittal, S.K., 2016. Components of adenovirus genome packaging. Front. Microbiol. 7, 1503.
Akusjarvi, G., 2008. Temporal regulation of adenovirus major late alternative RNA splicing. Front. Biosci. 13, 5006–5015.
Alexander, H.S., Huber, P., Cao, J., Krell, P.J., Nagy, E., 1998. Growth characteristics of fowl adenovirus type 8 in a chicken hepatoma cell line. J. Virol. Methods 74 (1), 9–14.
Beach, N.M., Duncan, R.B., Larsen, C.T., Meng, X.-J., Sriranganathan, N., Pierson, F.W., 2009. Comparison of 12 turkey hemorrhagic enteritis virus isolates allows prediction of genetic factors affecting virulence. J. Gen. Virol. 90 (8), 1978–1985.
Berk, A.J., et al., 2007. Adenoviridae: the viruses and their replication. In: 5 ed. In: Fields, B.N., Knipe, D.M., Howley, P.M. (Eds.), Fields Virology, 2 vols. Wolters Kluwer Health/Lippincott Williams & Wilkins, Philadelphia, pp. 2111–2148.
Biasiotto, R., Akusjarvi, G., 2015. Regulation of human adenovirus alternative RNA splicing by the adenoviral L4-33K and L4-22K proteins. Int. J. Mol. Sci. 16 (2), 2893–2912.
Cao, J.X., Krell, P.J., Nagy, E., 1998. Sequence and transcriptional analysis of terminal regions of the fowl adenovirus type 8 genome. J. Gen. Virol. 79 (10), 2507–2516.
Chardonnet, Y., Dales, S., 1970a. Early events in the interaction of adenoviruses with HeLa cells. I. Penetration of type 5 and intracellular release of the DNA genome. Virology 40 (3), 462–477.
Chardonnet, Y., Dales, S., 1970b. Early events in the interaction of adenoviruses with HeLa cells. II. Comparative observations on the penetration of types 1, 5, 7, and 12. Virology 40 (3), 478–485.
Davison, A., Harrach, B., 2011. Siadenovirus. In: Tidona, C., Darai, G. (Eds.), The Springer Index of Viruses. Springer, New York, pp. 49–56.
Davison, A.J., Wright, K.M., Harrach, B., 2000. DNA sequence of frog adenovirus. J. Gen. Virol. 81 (10), 2431–2439.
Davison, A.J., Benko, M., Harrach, B., 2003. Genetic content and evolution of adenoviruses. J. Gen. Virol. 84 (11), 2895–2908.
Dulbecco, R., Vogt, M., 1954. One-step growth curve of Western equine encephalomyelitis virus on chicken embryo cells grown in vitro and analysis of virus yields from single cells. J. Exp. Med. 99 (2), 183–199.
Fessler, S.P., Young, C.S.H., 1998. Control of adenovirus early gene expression during the late phase of infection. J. Virol. 72 (5), 4049–4056.
Henaff, D., Salinas, S., Kremer, E.J., 2011. An adenovirus traffic update: from receptor engagement to the nuclear pore. Future Microbiol. 6 (2), 179–192.
Iltis, J.P., Daniels, S.B., Wyand, D.S., 1977. Demonstration of an avian adenovirus as the causative agent of marble spleen disease. Am. J. Vet. Res. 38 (1), 95–100.
Jucker, M.T., McQuiston, J.R., van den Hurk, J.V., Boyle, S.M., Pierson, F.W., 1996. Characterization of the haemorrhagic enteritis virus genome and the sequence of the putative penton base and core protein genes. J. Gen. Virol. 77 (3), 469–479.
Katoh, H., Ohya, K., Kubo, M., Murata, K., Yanai, T., Fukushi, H., 2009. A novel budgerigar-adenovirus belonging to group II avian adenovirus of Siadenovirus. Virus Res. 144 (1-2), 294–297.
Kovács, E.R., Benkő, M., 2009. Confirmation of a novel siadenovirus species detected in raptors: partial sequence and phylogenetic analysis. Virus Res. 140 (1-2), 64–70.
Kovács, E.R., Benkő, M., 2011. Complete sequence of raptor adenovirus 1 confirms the characteristic genome organization of siadenoviruses. Infect. Genet. Evol. 11 (5), 1058–1065.
Kovács, E.R., Janoska, M., Dan, A., Harrach, B., Benkő, M., 2010. Recognition and partial genome characterization by non-specific DNA amplification and PCR of a new siadenovirus species in a sample originating from Parus major, a great tit. J. Virol.

Methods 163 (2), 262–268.
Kumar, P., van den Hurk, J., Ayalew, L.E., Gaba, A., Tikoo, S.K., 2015. Proteomic analysis of purified turkey adenovirus 3 virions. Vet. Res. 46, 79.
Mahsoub, H.M., 2015. Real Time PCR-Based Infectivity Assay and Characterization of Cell Surface Receptors for Turkey Hemorrhagic Enteritis Virus. Dissertation. Virginia Polytechnic Institute and State University.
Mahsoub, H.M., Evans, N.P., Beach, N.M., Yuan, L., Zimmerman, K., Pierson, F.W., 2017. Real-time PCR-based infectivity assay for the titration of turkey hemorrhagic enteritis virus, an adenovirus, in live vaccines. J. Virol. Methods 239, 42–49.
Nazerian, K., Fadly, A.M., 1982. Propagation of virulent and avirulent turkey hemorrhagic enteritis virus in cell culture. Avian Dis. 26 (4), 816–827.
Nazerian, K., Lee, L.F., Payne, W.S., 1991. Structural polypeptides of type II avian adenoviruses analyzed by monoclonal and polyclonal antibodies. Avian Dis. 35 (3), 572–578.
Ojkic, D., Krell, P.J., Nagy, E., 2002. Unique features of fowl adenovirus 9 gene transcription. Virology 302 (2), 274–285.
Payet, V., Arnauld, C., Picault, J.P., Jestin, A., Langlois, P., 1998. Transcriptional organization of the avian adenovirus CELO. J. Virol. 72 (11), 9278–9285.
Pierson, F.W., Fitzgerald, S.D., 2013. Hemorrhagic enteritis and related infections. In: 13 ed. In: Swayne, D.E., Glisson, J.R., McDougald, L.R., Nolan, L.K., Suarez, D.L., Nair, V. (Eds.), Diseases of Poultry, 1 vols. Wiley-Blackwell, Ames, Iowa, pp. 309–331.
Pierson, F.W., Larsen, C.T., Domermuth, C.H., 1996. The Production of colibacillosis in turkeys following sequential exposure to Newcastle disease virus or Bordetella avium, avirulent hemorrhagic enteritis virus, and Escherichia coli. Avian Dis. 40 (4), 837–840.
Pitcovski, J., Mualem, M., Rei-Koren, Z., Krispel, S., Shmueli, E., Peretz, Y., Gutter, B., Gallili, G.E., Michael, A., Goldberg, D., 1998. The complete DNA sequence and genome organization of the avian adenovirus, hemorrhagic enteritis virus. Virol 249 (2), 307–315.
Rautenschlein, S., Suresh, M., Sharma, J.M., 2000. Pathogenic avian adenovirus type II induces apoptosis in turkey spleen cells. Arch. Virol. 145 (8), 1671–1683.
Reddy, P., Idamakanti, N., Song, J., Lee, J., Hyun, B., Park, J., Cha, S., Bae, Y., Tikoo, S., Babiuk, L., 1998. Nucleotide sequence and transcription map of porcine adenovirus type 3. Virology 251, 414–426.
Rivera, S., Wellehan Jr., J.F., McManamon, R., Innis, C.J., Garner, M.M., Raphael, B.L., Gregory, C.R., Latimer, K.S., Rodriguez, C.E., Diaz-Figueroa, O., Marlar, A.B., Nyaoke, A., Gates, A.E., Gilbert, K., Childress, A.L., Risatti, G.R., Frasca Jr., S., 2009. Systemic adenovirus infection in Sulawesi tortoises (Indotestudo forsteni) caused by a novel siadenovirus. J. Vet. Diagn. Invest. 21 (4), 415–426.
Russell, W., 2000. Update on adenovirus and its vectors. J. Gen. Virol. 81 (2573), 2604.
Russell, W.C., 2009. Adenoviruses: update on structure and function. J. Gen. Virol. 90 (1), 1–20.
Saunders, G.K., Pierson, F.W., Hurk, J.Vvd., 1993. Haemorhagic enteritis virus infection in turkeys: a comparison of virulent and avirulent virus infections, and a proposed pathogenesis. Avian Pathol. 22 (1), 47–58.
Shu, L., Pettit, S.C., Engler, J.A., 1988. The precise structure and coding capacity of mRNAs from early region 2B of human adenovirus serotype 2. Virology 165 (2), 348–356.
Suresh, M., Sharma, J.M., 1995. Hemorrhagic enteritis virus induced changes in the lymphocyte subpopulations in turkeys and the effect of experimental immunodeficiency on viral pathogenesis. Vet. Immunol. Immunopathol. 45 (1–2), 139–150.
Suresh, M., Sharma, J.M., 1996. Pathogenesis of type II avian adenovirus infection in turkeys: in vivo immune cell tropism and tissue distribution of the virus. J. Virol. 70 (1), 30–36.
Tolin, S.A., Domermuth, C.H., 1975. Hemorrhagic enteritis of turkeys: electron microscopy of the causal virus. Avian Dis. 19 (1), 118–125.
van den Hurk, J.V., 1990. Propagation of group II avian adenoviruses in turkey and chicken leukocytes. Avian Dis. 34 (1), 12–25.
van den Hurk, J.V., 1992. Characterization of the structural proteins of hemorrhagic enteritis virus. Arch. Virol. 126 (1–4), 195–213.
Wellehan Jr., J.F., Greenacre, C.B., Fleming, G.J., Stetter, M.D., Childress, A.L., Terrell, S.P., 2009. Siadenovirus infection in two psittacine bird species. Avian Pathol. 38 (5), 413–417.
Wu, K., Guimet, D., Hearing, P., 2013. The adenovirus L4-33K protein regulates both late gene expression patterns and viral DNA packaging. J. Virol. 87 (12), 6739–6747.
Zhang, C.L., Nagaraja, K.V., Sivanandan, V., Newman, J.A., 1991. Identification and characterization of viral polypeptides from type-II avian adenoviruses. Am. J. Vet. Res. 52 (7), 1137–1141.